Structural, dielectric, magnetic, and nuclear magnetic resonance studies of multiferroic Y-type hexaferrites

H. Khanduri, M. Chandra Dimri, H. Kooskora, I. Heinmaa, G. Viola et al.

Citation: J. Appl. Phys. **112**, 073903 (2012); doi: 10.1063/1.4754532
View online: http://dx.doi.org/10.1063/1.4754532
View Table of Contents: http://jap.aip.org/resource/1/JAPIAU/v112/i7
Published by the American Institute of Physics.

Structural, dielectric, magnetic, and nuclear magnetic resonance studies of multiferroic Y-type hexaferrites

H. Khanduri,[1,2,a)] M. Chandra Dimri,[1] H. Kooskora,[1] I. Heinmaa,[1] G. Viola,[3] H. Ning,[3] M. J. Reece,[3] J. Krustok,[2] and R. Stern[1]
[1]*National Institute of Chemical Physics and Biophysics, Tallinn-12618, Estonia*
[2]*Tallinn University of Technology, Tallinn-19086, Estonia*
[3]*School of Engineering and Materials Science, Queen Mary University of London, Mile End Road, London E1 4NS, United Kingdom*

(Received 29 March 2012; accepted 24 August 2012; published online 1 October 2012)

The effect of strontium substitution on structural, magnetic, and dielectric properties of a multiferroic Y-type hexaferrite (chemical formula $Ba_{2-x}Sr_xMg_2Fe_{12}O_{22}$ with $0 \leq x \leq 2$) was investigated. Y-type hexaferrite phase formation was not affected by strontium substitution for barium, in the range $0 \leq x \leq 1.5$, confirmed by x-ray diffraction and Raman spectroscopy measured at room temperature. Two intermediate magnetic spin phase transitions (at tempertures T_I and T_{II}) and a ferrimagnetic-paramagnetic transition (at Curie temperature T_C) were identified from the temperature dependence of the magnetic susceptibility. Magnetic transition temperatures (T_I, T_{II}, and T_C) increased with increasing strontium content. Magnetic hysteresis measurements indicated that by increasing strontium concentration, the coercivity increases, while the saturation magnetization decreases. The ^{57}Fe NMR spectrum of the Y-type hexaferrite measured at 5 K and in zero magnetic field showed remarkable differences compared to that of other hexaferrites due to their different number of tetrahedral and octahedral iron sites. The temperature and frequency dependence of the dielectric permittivity evidenced broad peaks with frequency dispersion in correspondence of the Curie temperature. © *2012 American Institute of Physics*. [http://dx.doi.org/10.1063/1.4754532]

I. INTRODUCTION

Hexagonal ferrites are largely used in different types of electronic and microwave devices due to their versatile magnetic properties.[1–5] Hexaferrites are subdivided into six types, according to their chemical formula and structure, namely M-, W-, Y-, Z-, X-, and U-type.[6,7] Most hexaferrites have M-type structure as one of the basic units. This has the simplest structure among the other six variants and is composed of R and S blocks. The R block has the stoichiometry $BaFe_6O_{11}$, with five octahedral sites of two different types and one trigonal bipyramidal site. The S unit is formed by two formula units of Fe_3O_4 with the spinel structure containing two tetrahedral and four octahedral cation sites. Y-type hexaferrites are derived from S and T blocks.[7–9] The T unit has four layers with formula $Ba_2Fe_8O_{14}$, where Fe ions occupy two tetrahedral sites, and six octahedral sites of two different types (Fig. 1). Magnetic spin blocks stack along the c axis, with alternating large (μ_L) and small (μ_S) magnetic moments of opposite direction, produce collinear ferrimagnetism even at high temperatures exceeding room temperature. Decreasing the temperature, Y-type hexaferrites undergo transitions from a collinear ferrimagnetic phase to a proper-screw spin phase, and at lower temperature, from screw spin phase to a longitudinal conical spin phase (see Fig. 1).[10]

Y- and Z-types hexaferrites attracted large interest in recent years due to the observation of magnetoelectric effects,[9–13] the possibility of tailoring magnetic properties by varying doping and sintering conditions,[14] and the recent discovery of ferroelectricity.[9,10,15] Ferroelectricity in a Y-type hexaferrite system ($Ba_{0.5}Sr_{1.5}Zn_2Fe_{12}O_{22}$) was first reported by Kimura *et al.*[9] At ambient conditions and zero magnetic field, $Ba_{0.5}Sr_{1.5}Zn_2Fe_{12}O_{22}$ is a nonferroelectric insulator with noncollinear spin arrangement. In an applied magnetic field, it undergoes several phase transitions and some of the phases exhibit ferroelectricity induced by a critical magnetic field of 0.3–0.8 T.[9,16,17] Ferroelectricity was also observed in $Ba_2Mg_2Fe_{12}O_{22}$ and $Ba_2(Mg_{1-x}Zn_x)_2Fe_{12}O_{22}$ Y-type hexaferrites, where the critical magnetic field to induce the ferroelectricity was dramatically reduced to 30 mT.[10,18] Chun *et al.*[18] partially substituted Fe with Al in $Ba_{0.5}Sr_{1.5}Zn_2(Fe_{1-x}Al_x)_{12}O_{22}$ and successfully induced the ferroelectric phase at 1 mT.

In order to further explore the interesting properties of Mg_2Y hexaferrites ($Ba_2Mg_2Fe_{12}O_{22}$), we investigated the effect of strontium substitution on structure, magnetic transition temperatures, and dielectric behaviour of $Ba_{2-x}Sr_xMg_2Fe_{12}O_{22}$ ($0 \leq x \leq 2$), prepared by chemical solution method. Strontium was chosen because it has good solubility in Y-type barium hexaferrite, and it has also shown to improve the magnetic properties of Y-type hexaferrites.[19]

II. EXPERIMENTAL

Polycrystalline powder samples of $Ba_{2-x}Sr_xMg_2Fe_{12}O_{22}$ (with $x = 0$, 0.5, 1, 1.5, and 2) were prepared by chemical citrate solution method.[20,21] Initially, the aqueous solutions (0.5M) of $Ba(NO_3)_2$, $SrCO_3$, MgO, $Fe(NO_3)_3 \cdot 9H_2O$, and citric acid were prepared separately in deionised water. These solutions were mixed and the *p*H of the resulting solution was

a)Author to whom correspondence should be addressed. Electronic mail: himani.khanduri@gmail.com.

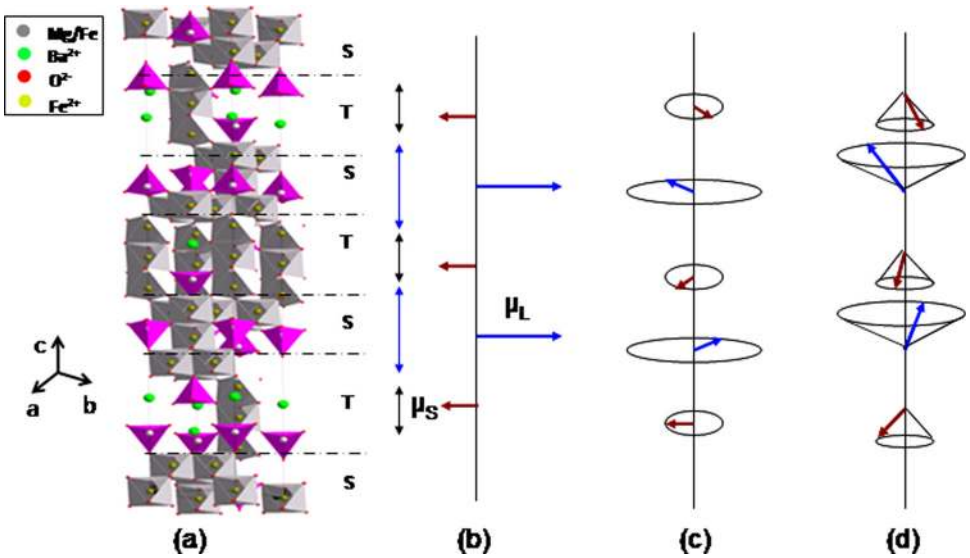

FIG. 1. (a) Schematic crystal structure of Y-type hexaferrite; (b) the ferrimagnetic structure consists of alternate stacks of two spin blocks with μ_L (larger magnetic moments) and μ_S (small magnetic moments) along c axis. (c) and (d) represent the proper screw structure and longitudinal conical spin order states respectively exhibited at lower temperatures.[10,11]

made neutral or slightly alkaline (pH = 7–8) by adding ammonia solution. The solution was heated on hot plate with constant stirring until auto-combustion. The resulting powders were heated at 500 °C for 3 h to remove the organic impurities. The powders were pressed in disc shape pellets and sintered at 1200 °C for 5 h in air.

Powder x-ray diffraction and Raman spectroscopy were used for phase identification. The x-ray diffraction was carried out using a Philips x-ray diffractometer. Raman spectroscopy (Horiba Jobin Yvon Labram HR 800) was performed at room temperature on sintered samples. Vibrating sample magnetometer (VSM, Quantum Design's 14T–PPMS) was used to measure the magnetic susceptibility and hysteresis loops of the sintered and crushed powder samples. The temperature dependence of magnetization was measured in a broad temperature range (10–850 K). Magnetic hysteresis loops were measured in the range 10–400 K. The solid state NMR (^{57}Fe) spectra were measured using the Fourier transform spin echo technique on Bruker AVANCE II NMR spectrometer. The spectra were recorded at T = 5 K in zero external field, because the signal was noisy and weak at room temperature. The excitation frequency was varied from 69 to 77 MHz in steps of 0.1 MHz to cover the full broad spectral range of lines corresponding to different typical crystallographic iron sites in hexaferrites. For the dielectric measurements, the disk shape pellets were coated with silver electrodes. The temperature dependence of the dielectric permittivity and loss was measured at various frequencies from 1 to 100 kHz using a precision LCR meter (Agilent, 4284A) connected to a high temperature tube furnace.

III. RESULTS AND DISCUSSION

A. Phase identification

Figure 2 shows the XRD patterns of the samples calcined at 1200 °C/5 h. The x-ray diffractograms reveal that samples $Ba_{2-x}Sr_xMg_2Fe_{12}O_{22}$ (with x = 0, 0.5, 1, 1.5) have pure Y-type hexagonal structure, whereas $Sr_2Mg_2Fe_{12}O_{22}$ (x = 2) does not exhibit single phase Y-type structure and was therefore not examined in details in the present study. This is consistent with previous structural studies on Zn_2Y hexaferrites,[19] where the maximum solubility of strontium in the $Ba_{2-x}Sr_xZn_2Fe_{12}O_{22}$ ferrite was found to be about 1.8, and complete substitution of Ba^{2+} by Sr^{2+} prevented the Y-type phase formation.

Lattice parameters of $Ba_{2-x}Sr_xMg_2Fe_{12}O_{22}$ (with x = 0, 0.5, 1, 1.5) calculated and listed in Table I confirmed Y-type hexaferrite phase. The value of lattice parameter "a" decreased with the rise of Sr content, since the ionic radius of Sr^{2+} (1.32 Å) is smaller compared to Ba^{2+} (1.49 Å). The c/a ratio increased with increasing strontium content.

The Raman spectra measured at room temperature in Fig. 3 also confirm that $Ba_{2-x}Sr_xMg_2Fe_{12}O_{22}$ samples exhibit a hexaferrite structure.[22–25] In our knowledge, there are not many Raman studies on Y-type hexaferrites, except a recent publication on Zn_2Y hexaferrite.[26] Raman peaks become broader with the increase of the value of x from 0 to 1.5 (Fig. 3). Changes in chemical composition, atomic radii, valence, bond length, cell size, and magnetic order might lead to the broadening of Raman peaks.[27] In our samples,

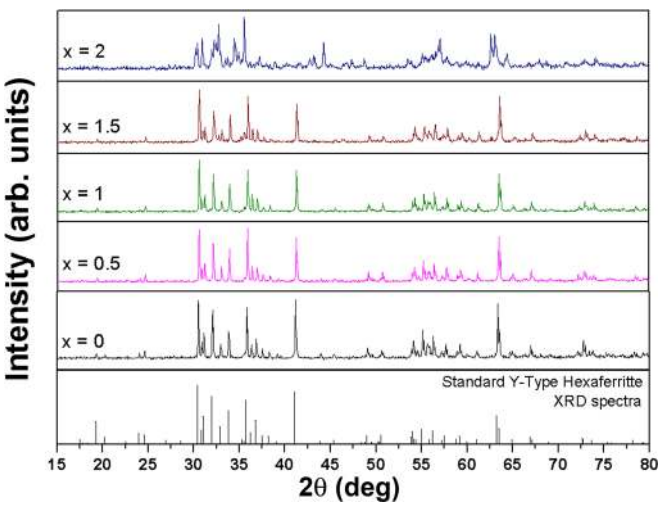

FIG. 2. X-ray diffraction patterns of $Ba_{2-x}Sr_xMg_2Fe_{12}O_{22}$ powder samples.

TABLE I. Lattice parameters for different Sr concentration in the $Ba_{2-x}Sr_xMg_2Fe_{12}O_{22}$ samples (with estimated errors).

Value of x in $Ba_{2-x}Sr_xMg_2Fe_{12}O_{22}$	a (Å) (1%)	c (Å) (0.5%)	c/a
0	5.866	43.2683	7.376
0.5	5.8548	43.3514	7.404
1	5.8436	43.2799	7.406
1.5	5.8436	43.2799	7.406

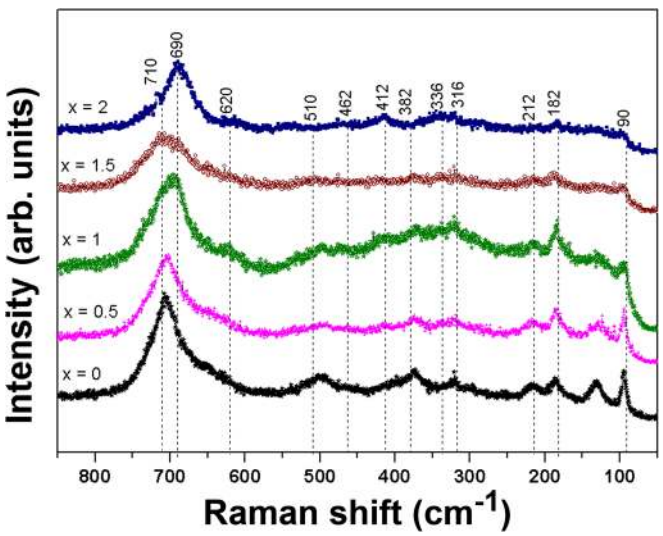

FIG. 3. Raman spectra of $Ba_{2-x}Sr_xMg_2Fe_{12}O_{22}$ bulk samples.

peak broadening may be related to changes in magnetic structure on strontium substitution.

B. Magnetic studies

The magnetic phase transition temperatures in $Ba_{2-x}Sr_xMg_2Fe_{12}O_{22}$ for different strontium content (x = 0, 0.5, 1, 1.5) were determined from the temperature dependence of magnetic susceptibility measured in an applied magnetic field of 0.1 T (Fig. 4). The ferrimagnetic-paramagnetic transition (Curie temperature, T_C) was identified as the temperature where the magnetic susceptibility significantly dropped. The two visible susceptibility peaks in correspondence of temperatures T_I and T_{II} (Fig. 4) are associated with the consecutive magnetic spin transitions. Decreasing the temperature, the magnetic order changes from collinear ferrimagnetic to a proper-screw spin phase at transition temperature II, and from screw spin phase to a longitudinal conical spin phase around transition temperature I (see also Fig. 1), as recently suggested for $Ba_2Mg_2Fe_{12}O_{22}$ (x = 0) based on neutron diffraction.[28,30] The magnetic transition temperatures of different samples of $Ba_{2-x}Sr_xMg_2Fe_{12}O_{22}$ are given in Table II. It can be seen that all the magnetic transition temperatures increase with increasing Sr content.

Figure 5 shows the magnetic hysteresis loops of $Ba_{2-x}Sr_xMg_2Fe_{12}O_{22}$ measured at 300 K for different strontium content (x = 0, 0.5, 1, 1.5). Coercivity was found to be increased with strontium concentration (for x = 1.5, the coercivity is two times larger than in case of x = 0). Similar behaviour in coercivity was also found by other research groups on Sr substitution in Y-type hexaferrites.[19,29] The ground state magnetic structure of these hexaferrites $\{(BaSr)_2Mg_2Fe_{12}O_{22}$, $(BaSr)_2Zn_2Fe_{12}O_{22}\}$ is composed of alternating stacking of the L and S blocks along the c axis.[31] The magnetic moments of Fe sites lying in the ab plane are in collinear ferrimagnetic structures, within these blocks. The Sr-free sample shows the collinear ferrimagnetic order at room temperature, whereas the antiferromagnetic order increased with the increase in Sr content. The enhancement in antiferromagnetic order for higher concentration (x = 1.5) results in increased coercivity, whereas the composition x = 1 shows slight decrease in coercivity, possibly due to an

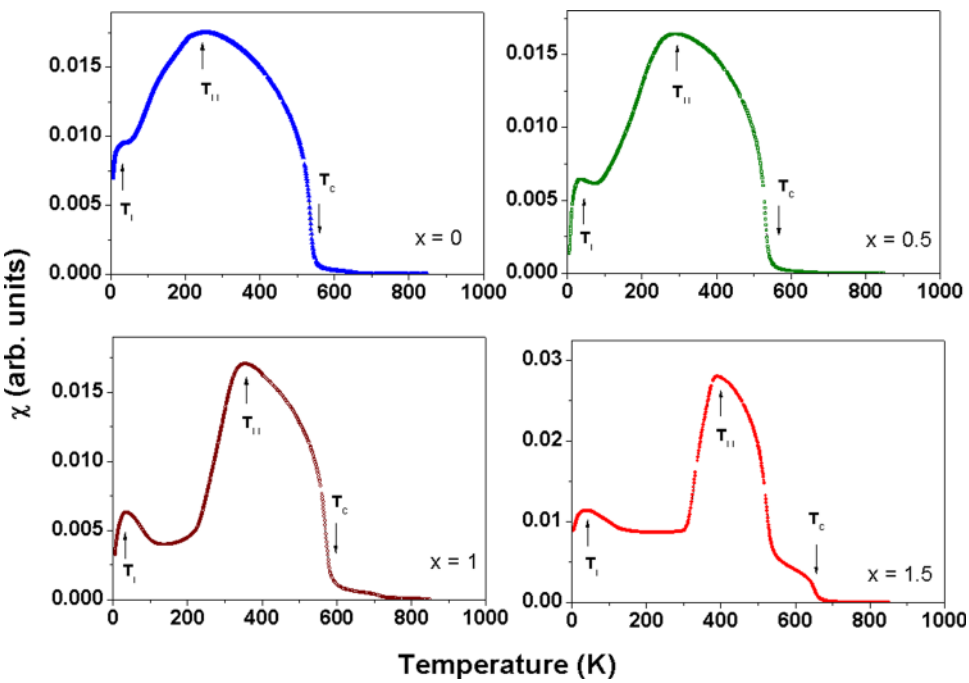

FIG. 4. Temperature dependence of susceptibility for $Ba_{2-x}Sr_xMg_2Fe_{12}O_{22}$ samples.

TABLE II. Coercivities and magnetic transition temperatures (with average estimated errors) of the powder samples of $Ba_{2-x}Sr_xMg_2Fe_{12}O_{22}$.

Value of x in $Ba_{2-x}Sr_xMg_2Fe_{12}O_{22}$	Coercivity H_c (Oe)	Transition temperatures (K)		
		T_I (±5 K)	T_{II} (±10 K)	T_C (K) (±5 K)
0	100	20	260	550
0.5	150	30	290	550
1	100	35	355	590
1.5	200	40	390	670

intermediate phase (between proper-screw and conical spin phase) and magnetic frustrations existing at this composition. Enhancement in coercivity in antiferromagnetic phase is understandable, because it needs higher demagnetizing fields as compared to ferrimagnetic material. At room temperature, $Ba_{2-x}Sr_xMg_2Fe_{12}O_{22}$ samples with compositions $x = 0$ and $x = 0.5$ are still in collinear ferrimagnetic phase (show single ferrimagnetic loop), while samples with $x = 1$ and $x = 1.5$ have entered already in the screw spin phase (showed triple loops). The abnormal triple loops are related to the changes in the magnetic phases and intermediate phases produced by strontium substitution in $Ba_{2-x}Sr_xMg_2Fe_{12}O_{22}$ samples. Kimura *et al.* had also observed the phase change from collinear ferrimagnetic to antiferromagnetic state, with other intermediate phases, depending on Sr substitution for barium ions in Zn_2Y hexaferrites.[9] Our $Ba_{2-x}Sr_xMg_2Fe_{12}O_{22}$ samples with higher strontium concentration ($x = 1$ and 1.5) exhibit an intermediate magnetic phase in between proper screw spin phase and conical spin phase at room temperature. This intermediate phase could be responsible for multistage abnormal hysteresis loop. This kind of loops has been observed in $Ba_2Mg_2Fe_{12}O_{22}$ samples (at 10 K) by Sagayama *et al.*,[30] and they attributed it to the phase transition of the magnetic structure, which was supported by neutron diffraction studies at low temperatures.[30]

In order to study the magnetic behaviour of the different magnetic phases, magnetic hysteresis loops of $Ba_{0.5}Sr_{1.5}Mg_2Fe_{12}O_{22}$ were measured at selected representative temperatures in the range 10–400 K (Fig. 6). Figs. 6(a) and 6(b) show the magnetic hysteresis at 10 and 30 K, respectively, where the conical spin phase is exhibited. In the range 200–350 K, the sample has a screw spin phase and it shows triple M-H loops (Figs. 6(c)–6(e)). At 400 K, $Ba_{0.5}Sr_{1.5}Mg_2Fe_{12}O_{22}$ sample has collinear ferrimagnetic order and the magnetic hysteresis curve shows the typical ferrimagnetic behaviour (Fig. 6(f)).

C. NMR measurements on $Ba_2Mg_2Fe_{12}O_{22}$

The ^{57}Fe NMR spectrum of $Ba_2Mg_2Fe_{12}O_{22}$ measured at 5 K in zero applied magnetic field is shown in Fig. 7. The NMR spectrum is noisy and broad, consistent with previous NMR measurements on Y-type hexaferrites.[32] Y-type hexaferrites have six sublattice sites ($6c_{IV}$, $3a_{VI}$, $18h_{VI}$, $6c_{VI}$, $6c_{IV*}$, and $3b_{VI}$),[32] which could not be distinguished in our NMR spectrum. In case of M-type[33] and U-type[34] barium hexaferrites, the NMR

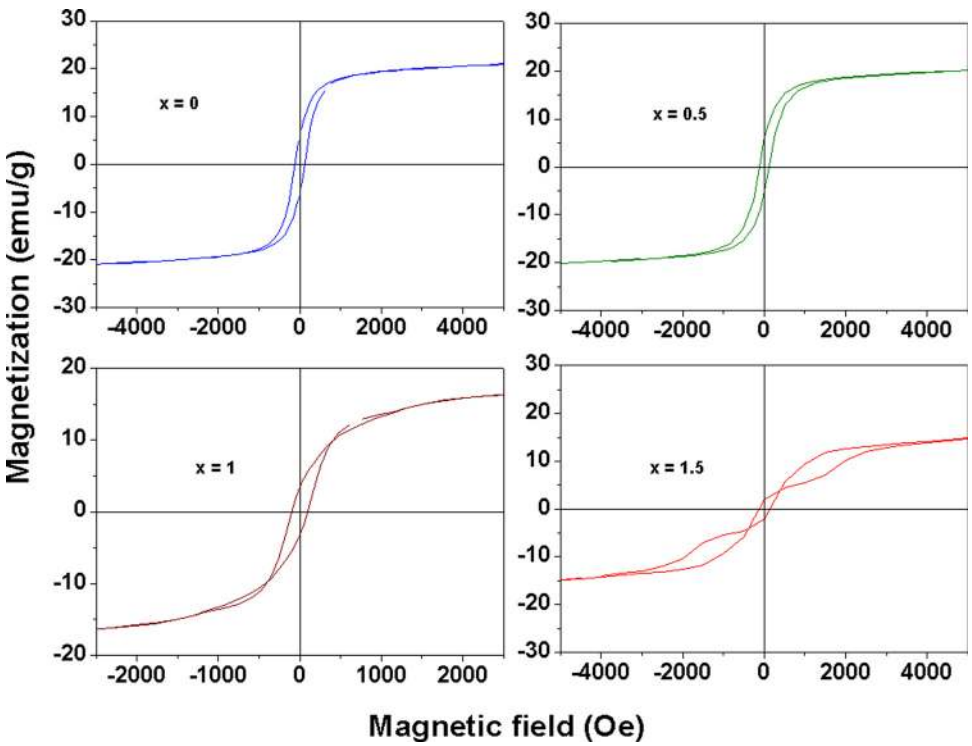

FIG. 5. Hysteresis loops measured at 300 K of $Ba_{2-x}Sr_xMg_2Fe_{12}O_{22}$ samples.

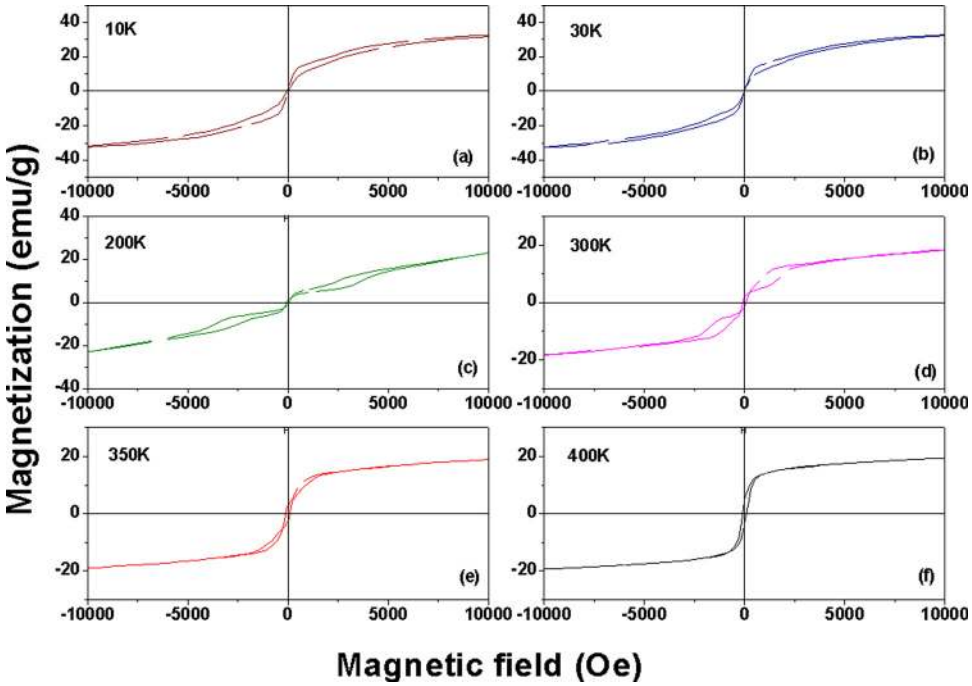

FIG. 6. Hysteresis loops of the powder samples of $Ba_{0.5}Sr_{1.5}Mg_2Fe_{12}O_{22}$ measured at (a) 10 K, (b) 30 K, (c) 200 K, (d) 300 K, (e) 350 K, and (f) 400 K.

spectra consist of five peaks relative to the different lattice iron sites (12 k, $4f_{IV}$, 2a, $4f_{VI}$, and 2b in M-type and 12 k, $8f_{IV}$, 4a, $4f_{VI}$, and 2b in U-type hexaferrites). This unresolved spectrum is probably due to a number of different crystallographic (tetrahedral and octahedral) iron sites in the Y-type structure (see Fig. 1). The other reason of broadning may be related to its different magnetic order, because our Y-type hexaferrite samples are in conical spin order at this temperature (5 K), whereas M- and U-type hexaferrites are usually in collinear ferrimagnetic states at that temperature resulting in well resolved NMR spectra.

D. Dielectric studies

Figure 8 shows the temperature and frequency dependence of the dielectric permittivity ε_r and loss ($\tan\delta$) of

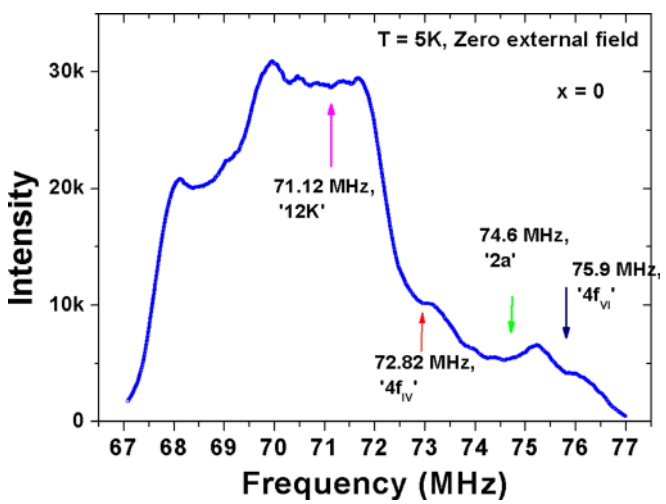

FIG. 7. ^{57}Fe NMR spectrum of $Ba_2Mg_2Fe_{12}O_{22}$ (x = 0) powder sample measured in zero field at 5 K. The expected lines of different iron sites as observed in M-type spectra are indicated by arrows at different frequencies.

$Ba_{2-x}Sr_xMg_2Fe_{12}O_{22}$. High dielectric loss is consistent with previous dielectric characterization on Y-type hexaferrites.[35] The dielectric permittivity exhibits very broad peaks in the range 430–680 K (Figs. 8(a)–8(d)). The broadness and position of the peaks changed with strontium content, but no clear trend could be assigned. It is likely that these peaks are associated with the Curie (ferrimagnetic-paramagnetic) transition in the range 550–670 K as previously identified from our magnetic susceptibility data (see Table II). In addition, these peaks showed pronounced frequency dispersion, with the maximum shifting to higher temperature with increasing frequency. Frequency dependent peaks in the dielectric permittivity around the magnetic transition temperatures were also observed in other magnetic systems, such as bilayer manganite ($Pr(Sr_{0.1}Ca_{0.9})_2Mn_2O_7$)[36] and hexagonal ABX_3-type antiferromagnets.[37] In the bilayer manganite, it was observed that the broad anomaly around the Curie temperature had an intrinsic capacitive nature, which was also responsible for the frequency dispersion in the dielectric permittivity.[36] For the hexagonal ABX_3-type antiferromagnets, the dielectric anomalies and the strong frequency dispersion observed in $CsCoBr_3$ and the weaker dispersion in $RbCoBr_3$ were attributed to spin-lattice interaction.[37] Our results suggest that in Y-type hexaferrite too, the perturbation of the magnetic order during heating produces frequency dependent broad peaks in the dielectric constant. This indicates that the dielectric properties are influenced by the magnetic state. The dielectric loss peaks shown in Figs. 8(a)–8(d), also attributed to the transformation of the magnetic order.

An additional anomaly in the dielectric permittivity was observed at higher temperatures in the range 820–890 K, represented by broad or narrower peaks (see out-set of Figs. 8(a)–8(d)). The broadness and position of the peaks did not show any clear trend with strontium content. The position of the permittivity peaks at high temperatures (above 820 K) did not change with varying the frequency. This normally

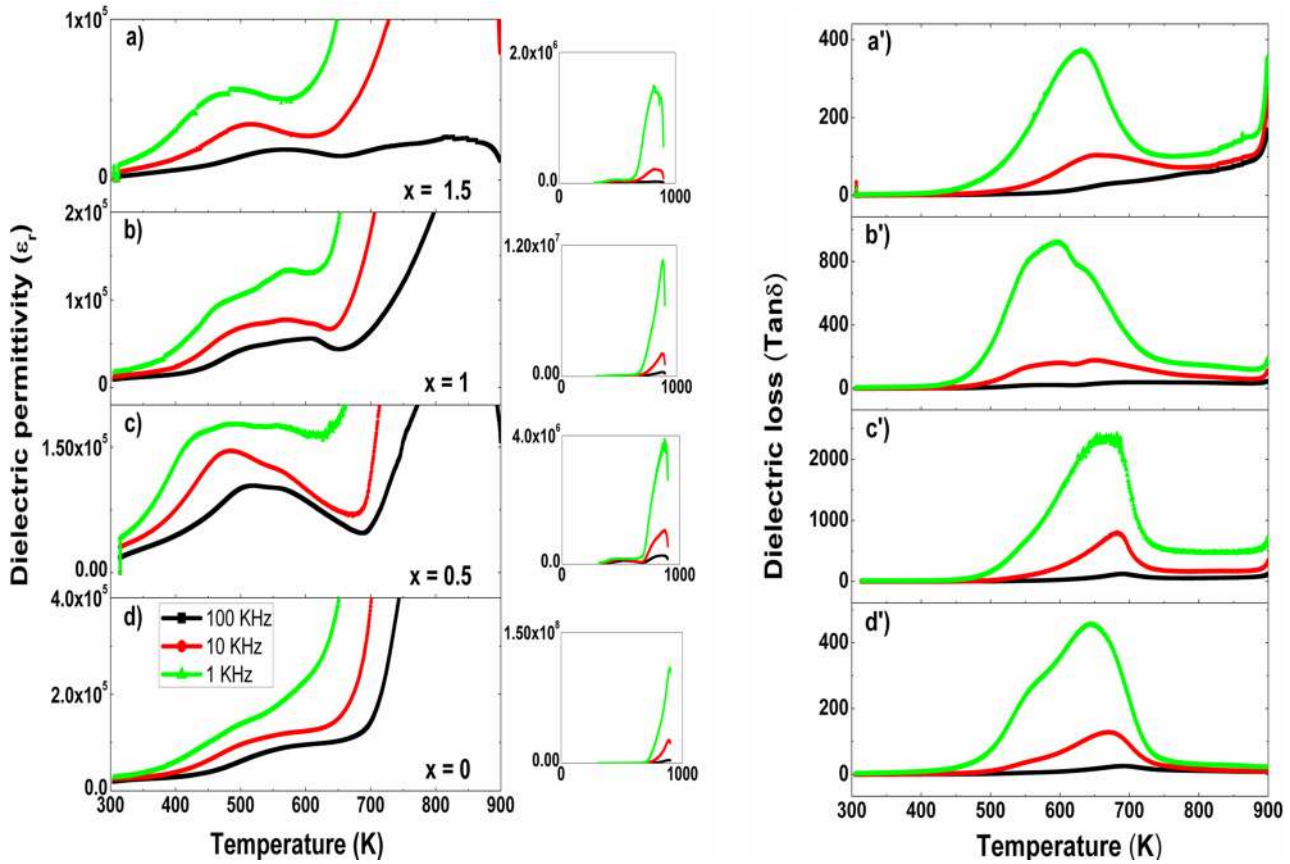

FIG. 8. Temperature dependence of the dielectric permittivity ε_r and dielectric loss (tanδ) of $Ba_{2-x}Sr_xMg_2Fe_{12}O_{22}$ samples measured at different frequencies.

occurs in correspondence of structural modifications, suggesting that the dielectric constant peaks observed probably indicate a phase transition.

IV. SUMMARY AND CONCLUSION

$Ba_{2-x}Sr_xMg_2Fe_{12}O_{22}$ samples synthesized by chemical citrate method have single phase Y-type hexaferrite structure in the compositional range $0 \leq x \leq 1.5$. Strontium substitution alters the magnetic phase transition temperatures and magnetic hysteresis behaviour. Intermediate spin phase transition temperatures and the Curie temperature (ferrimagnetic-paramagnetic phase transition) shifted to higher temperatures with increasing strontium content. Saturation magnetization decreases and coercivity increases with increasing Sr substitution for Ba ions. ^{57}Fe NMR spectrum measured at 5 K and in zero magnetic field was found to be broad for the $Ba_2Mg_2Fe_{12}O_{22}$ hexaferrite due to a more complex structure when compared to the well resolved NMR spectra for M-type hexaferrites. Broad and frequency dependent peaks were observed in the dielectric permittivity around the Curie temperature, evidencing that a change in the magnetic order affects the dielectric properties.

ACKNOWLEDGMENTS

This work was financially supported by the Estonian Science Foundation (Grant Nos.: ETF 8440, MJD 65), and the Estonian targeted financial Grant Nos. SF0690029s09 and SF0690034s09. One of the authors, Himani Khanduri thanks the DORA program (Estonian Science Foundation) for her doctoral fellowship.

[1]V. R. K. Murthy, S. Sundaram, and B. Vishwanathan, *Microwave Materials* (Narosa Publishing House, New Delhi, 1993).
[2]A. Ghasemi, A. Hossienpour, A. Morisako, A. Saatchi, and M. Salehi, J. Magn. Magn. Mater. **302**, 429 (2006).
[3]C. Wang, L. Li, J. Zhou, X. Qi, and Z. Yue, J. Mater. Sci.: Mater. Electron. **13**, 713 (2002).
[4]H.-S. Cho and S.-S. Kim, IEEE Trans. Magn. **35**, 3151 (1999).
[5]S. Sugimoto, S. Kondo, K. Okayama, H. Nakamura, D. Book, T. Kagotani, M. Homma, H. Ota, M. Kimura, and R. Sato, IEEE Trans. Magn. **35**, 3154 (1999).
[6]J. P. Jakubovics, "Magnetism and Magnetic Materials," 2nd Ed. (Institute of Materials, London, 1994).
[7]J. Smith and H. P. J. Wijn, *Ferrites* (Philips Technical Library, Eindhoven, The Netherlands, 1959), pp. 177–190, 285.
[8]U. Ozgur, Y. Alivov, and H. Morkoc, J. Mater. Sci.: Mater. Electron. **20**, 789 (2009).
[9]T. Kimura, G. Lawes, and A. P. Ramirez, Phys. Rev. Lett. **94**, 137201 (2005).
[10]S. Ishiwata, Y. Taguchi, H. Murakawa, Y. Onose, and Y. Tokura, Science **319**, 1643 (2008).
[11]S. Ishiwata, Y. Taguchi, Y. Tokunaga, H. Murakawa, Y. Onose, and Y. Tokura, Phys. Rev. B **79**, 180408(R) (2009).
[12]N. Kida, S. Kumakura, S. Ishiwata, Y. Taguchi, and Y. Tokura, Phys. Rev. B **83**, 064422 (2011).
[13]N. Kida, D. Okuyama, S. Ishiwata, Y. Taguchi, R. Shimano, K. Iwasa, T. Arima, and Y. Tokura, Phys. Rev. B **80**, 220406(R) (2009).
[14]Y. Bai, J. Zhou, Z. Gui, and L. Li, Mater. Chem. Phys. **98**, 66 (2006).
[15]Y. Kitagawa, Y. Hiraoka, T. Honda, T. Ishikura, H. Nakamura, and T. Kimura, Nature Mater. **9**, 797 (2010).
[16]N. Momozawa, Y. Yamaguchi, H. Takei, and M. Mita, J. Phys. Soc. Jpn. **54**, 3895 (1985).

[17]S. Utsumi, D. Yoshiba, and N. Momozawa, J. Phys. Soc. Jpn. **76**, 034704 (2007).
[18]S. H. Chun, Y. S. Chai, Y. S. Oh, D. Jaiswal-Nagar, S. Y. Haam, I. Kim, B. Lee, D. H. Nam, K.-T. Ko, J.-H. Park, J.-H. Park, J.-H. Chung, and K. H. Kim, Phys. Rev. Lett. **104**, 037204 (2010).
[19]Y. Bai, J. Zhou, Z. Gui, and L. Li, J. Am. Ceram. Soc. **88**(2), 318 (2005).
[20]M. C. Dimri, R. Stern, S. C. Kashyap, K. P. Bhatti, and D. C. Dube, Phys. Status Solidi A **206**(2), 270 (2009).
[21]M. C. Dimri, S. C. Kashyap, and D. C. Dube, Ceram. Int. **30**, 1623 (2004).
[22]W. Y. Zhao, P. Wei, W. Wang, and Q. J. Zhang, J. Appl. Phys. **103**, 063902 (2008).
[23]P. B. Braun, Philips Res. Rep. **12**, 491 (1957).
[24]M. S. Chen, Z. X. Shen, X. Y. Liu, and J. Wang, J. Mater. Res. **15**, 483 (2000).
[25]J. Kreisel, G. Lucazeau, and H. Vincent, J. Solid State Chem. **137**, 127 (1998).
[26]S. Kamba, V. Goian, M. Savinov, E. Buixaderas, D. Nuzhnyy *et al.*, J. Appl. Phys. **107**, 104109 (2010).
[27]J. Kreisel, G. Lucazeau, and H. Vincent, J. Raman Spectrosc. **30**(2), 115 (1999).
[28]S. Ishiwata, D. Okuyama, K. Kakurai, M. Nishi, Y. Taguchi, and Y. Tokura, Phys. Rev. B **81**, 174418 (2010).
[29]X. Fang, B. Yang, A. Fen, and Q. Li-Jie, Chin. Phys. B **17**(12), 4652 (2008).
[30]H. Sagayama, K. Taniguchi, N. Abe, T. H. Arima, Y. Nishikawa, S. I. Yano, Y. Kousaka, J. Akimitsu, M. Matsuura, and K. Hirota, Phys. Rev. B **80**, 180419(R) (2009).
[31]T. Kimura, Annu. Rev. Condens. Matter Phys. **3**, 93 (2012).
[32]G. Albanese, J. Phys. Colloq. **38**, C1–85 (1977).
[33]R. L. Streever, Phys. Rev. **186**(2), 285 (1969).
[34]M. C. Dimri, H. Khanduri, H. Kooskora, E. Joon, I. Heinmaa, and R. Stern, J. Magn. Magn. Mater. **323**(16), 2210 (2011).
[35]A. M. Abo El Atta and S. M. Attia, J. Magn. Magn. Mater. **257**, 165 (2003).
[36]B. Ghosh, D. Bhattacharya, A. K. Raychaudhuri, and S. Arumugam, J. Appl. Phys. **105**, 123914, (2009).
[37]K. Morishita, K. Iio, T. Mitsui, and T. Kato, J. Magn. Magn. Mater. **226**, 579 (2001).